

GRANT  
1N-89-CR  
7279  
P-20

X-RAY ABSORPTION BY DARK NEBULAE  
(HEAO-2 Guest Investigator Program)

W. T. Sanders, Principal Investigator  
Department of Physics  
University of Wisconsin  
Madison, Wisconsin 53706

Final Report  
NASA Grant NAG 8-401

April 19, 1991

(NASA-CR-188076) X RAY ABSORPTION BY DARK  
NEBULAE (HEAO-2 GUEST INVESTIGATOR PROGRAM)  
Final Report (Wisconsin Univ.) 20 p

CSCL 03A

63/89

N91-21011

Unclas  
0007279

## I. INTRODUCTION

This report describes a study of data obtained from the Imaging Proportional Counter (IPC) x-ray detector aboard the HEAO-2 satellite (*Einstein Observatory*). The research project involved a search for absorption of diffuse low energy x-ray background emission by galactic dark nebulae. The research proposed fell into Category B, described in the NASA Space Science Notice of July 7, 1978, in that I proposed to collaborate with a HEAO-2 Consortium Scientist, Dr. Frank Marshall of the NASA Goddard Space Flight Center (GSFC), and proposed to utilize a data set, sequence numbers I7227-I7240, from the HEAO-2 satellite. This data set was to have been collected in response to the GSFC observing proposal titled "IPC Observations of Dark Nebulae," which requested a 10,000 second observation using the IPC toward each of 14 targets selected from the Lynds (1962) catalogue of dark nebulae.

In addition, this research project was augmented to include the work proposed in a separate *Einstein* guest investigator proposal submitted at the same time but not funded. That work involved follow-up observations, using the *Einstein Observatory* High Resolution Imager (HRI), of the serendipitously discovered sources found in two earlier *Einstein* guest investigator projects that I was involved with. Sequence number H9191 was a follow up observation of the serendipitous source found in sequence I3809 (the Coalsack Nebula), and H9192 was a follow up observation of the serendipitous source found in I3124 (9 Sgr).

## II. SCIENTIFIC BACKGROUND

The x-ray background in the energy interval 0.1-0.28 keV (C band) is believed to originate almost entirely ( $> 95\%$ ) from a million degree interstellar plasma surrounding the Sun and extending to distances of order 50-100 parsecs in all directions. In the higher energy interval, 0.5-1.2 keV (M band), this local hot plasma is believed to make only a small contribution ( $\leq 5\%$ ) and most of the x-rays are thought to originate at distances greater than 100 parsecs. It is not certain what fraction of the M band emission arises from more distant interstellar plasmas, or from numerous weak stellar sources, or from a galactic halo, or from outside the galaxy entirely, but some contribution from each of these sources is likely.

The goal of the research proposed here was to test the commonly accepted picture that the bulk of the C band emission originates locally, closer than a few hundred parsecs, and the bulk of the M band emission originates farther away than a few hundred parsecs. The idea was to look for evidence of absorption of the diffuse background radiation by nearby interstellar clouds. The spectrum of the diffuse x-rays detected from the direction of each of the clouds was to be compared to spectra from directions not towards that cloud but within that same image. The picture described above predicts the C band intensity to be the same for each spectrum taken from a given image, but predicts the M band intensity in directions toward the cloud to be less than that measured in directions away from the cloud.

The secondary goal of the research sponsored by this grant was to pursue the identification of two of the serendipitous sources found in the images of previous *Einstein* observations.

### III. RESULTS

#### A. Dark Clouds

In early 1981, the Einstein Observatory began to experience failures of its gyroscopes. The reduced operational capacity of the spacecraft and the limited remaining mission lifetime precluded the observation of all of the planned targets of the observing program. Of the 14 dark nebulae requested by the GSFC proposal, only two, L409 (I7229) and L1605 (I7237), were observed before *Einstein* reentered the atmosphere.

##### 1. I7237

Observation sequence number I7237 corresponds to the Lynds dark cloud L1605, which is also part of the molecular cloud complex that accompanies Mon OB1. The observation of L1605 was centered at  $6^{\text{h}} 30^{\text{m}}$ ,  $10^{\circ} 40'$  (1950), galactic coordinates ( $201^{\circ}$ ,  $1^{\circ}$ ).

Before beginning the analysis of this field, the I7237 data were cleaned according to the procedures developed for the analysis of the Coalsack data under an earlier *Einstein* guest investigator grant. In summary, the counts in the lowest energy bins are examined as a function of time, and all time intervals when the integrated count rate from the whole field in those bins rises more than two sigma above its minimum value are eliminated.

Within the L1605 field, two rectangular regions were identified, each 15.20 arcminutes in R.A. by 10.93 arcminutes in Dec. In this direction on the sky, these dimensions correspond to  $\pm 31^{\text{s}}$  in R.A. and  $\pm 5'28''$  in Dec. The "On-Cloud" region was centered on a dense part of the L1605 cloud at  $6^{\text{h}} 30^{\text{m}} 17^{\text{s}}$ ,  $10^{\circ} 29' 48''$  and the "Off-Cloud" region was centered away from the dense part of the cloud at  $6^{\text{h}} 29^{\text{m}} 36^{\text{s}}$ ,  $10^{\circ} 51' 8''$ . To the eye, no difference is apparent in the number of x-ray counts between the Off-Cloud region and the

On-Cloud region - no shadow of the x-ray background cast by the interstellar cloud is seen. Figure 1 shows an image of the field, the Off-Cloud region, the On-Cloud region and the pulse height distribution from each region.

Quantitatively, the difference in the total number of counts between the Off-Cloud region and the On-Cloud region is  $\Delta = 1776 - 1868 = -92 \pm 60$  counts, a value not significantly different from zero. If anything, it indicates not that the cloud is absorbing x-rays, but it may be emitting them - as though it contains a population of low luminosity sources, new-born stars, perhaps. Alternatively, there may be some peculiarity of the proportional counter detector that causes one particular region of the counter to have an intrinsically higher rate than another.

To investigate this possibility, six comparison fields were defined: five observations of isolated stars where no x-ray sources were detected and where there are no interstellar clouds (I5041, I5046, I5064, I5067, and I5070), and a long exposure taken with the aluminum filter in place (I10754). For each of these observations, the x-ray counts detected in the parts of the proportional counter that correspond to the Off-Cloud and to the On-Cloud regions of the I7237 observation were extracted. Table 1 tabulates the total number of counts detected in these parts of the counter for the comparison observations and for I7237. There is no evidence for any systematic difference in the number of counts between the two regions of the proportional counter.

Finally, the pulse height distributions of the two regions are compared, both for the I7237 data and for the comparison regions. For this comparison to be useful, only those comparison fields that have a proportional counter gain close to that of I7237 can be used, even though the data are supposed to be in "pulse height independent" (PI) bins. I7237 is a "high gain" observation (ALP=16), so comparison fields I5046, I5064, and I5070, which are low gain fields (ALP=12-13), cannot be used, but I5041, I5067 and I10754 can be used.

Table 1 - Counts from the I7237 Off-Cloud and On-Cloud Regions of the Proportional Counter for 6 Comparison Fields

Sequence	Off-Cloud	On-Cloud	Difference
I5041	811	796	15 ± 40
I5046	887	889	-2 ± 42
I5064	836	836	0 ± 41
I5067	1022	1044	-22 ± 45
I5070	568	568	0 ± 34
I10754 (filter)	5415	5396	19 ± 104
<b>All Comparison Fields</b>	<b>9539</b>	<b>9529</b>	<b>10 ± 138</b>
<b>I7237</b>	<b>1776</b>	<b>1868</b>	<b>-92 ± 60</b>

Figure 2 shows the pulse height distributions from the I7237 (L1605) On-Cloud and Off-Cloud regions, and Figure 3 shows the pulse height distributions for the high-gain comparison fields. It is not obvious that there is a significant difference in the Off-Cloud/On-Cloud pulse height distributions from L1605. If anything, the L1605 On-Cloud spectrum shows excess counts in channels 3-5 (M band), whereas the comparison fields have the Off-Cloud region showing a slight excess in channels 3-5. As was suggested earlier, this perhaps is indicative of emission from the very young stars in and toward the L1605 cloud, but provides no evidence for absorption of the diffuse x-ray background in this direction.

## 2. I7229

Observation sequence number I7229 corresponds to the Lynds dark cloud L409. The observation of L409 was centered at 18<sup>h</sup> 39<sup>m</sup>, -13° 30' (1950), galactic coordinates (20°, -4°). Before beginning the analysis of this field, the I7229 data were cleaned according to the procedures summarized earlier for observation I7237.

Within the L409 field, two rectangular regions were identified, each 10.93 arcminutes in R.A. by 15.20 arcminutes in Dec. In this direction on the sky, these dimensions correspond to  $\pm 22.5^{\text{S}}$  in R.A. and  $\pm 7'36''$  in Dec. The "On-Cloud" region was centered on a dense part of the L409 cloud at  $18^{\text{h}} 39^{\text{m}} 42^{\text{S}}$ ,  $-13^{\circ} 35' 56''$  and the "Off-Cloud" region was centered away from the dense part of the cloud at  $18^{\text{h}} 38^{\text{m}} 32^{\text{S}}$ ,  $-13^{\circ} 23' 8''$ . To the eye, no difference is apparent in the number of x-ray counts between the Off-Cloud region and the On-Cloud region - no shadow of the x-ray background cast by the interstellar cloud is seen. Figure 4 shows an image of the field, the Off-Cloud region (labeled Region 3), the On-Cloud region (labeled Region 2) and the pulse height distribution from each region.

To be quantitative, the difference in the total number of counts between the Off-Cloud region and the On-Cloud region is  $\text{DELTA} = 1641 - 1560 = 81 \pm 57$  counts, a value not significantly different from zero. It indicates that there is a possibility that the cloud is absorbing x-rays, so the behavior of the comparison fields will be checked. The same six comparison fields that were used in the I7237 analysis were used here, only this time the areas of the proportional counter corresponding to the I7229 Off-Cloud and On-Cloud regions were used. Table 2 tabulates the total number of counts detected in these parts of the counter for the comparison observations and for I7229. In this case, the comparison fields show that there is a significant instrumental excess in the Off-Cloud region of the proportional counter, which predicts that the I7229 observation will show an Off-Cloud excess of  $\approx 60$  counts. Since the data show an I7229 Off-Cloud excess of 81 counts, it is consistent with the L409 cloud showing neither an excess of counts, nor a deficit as might be expected by absorption of a diffuse background intensity.

Table 2 - Counts from the I7229 Off-Cloud and On-Cloud Regions of the Proportional Counter for 6 Comparison Fields

Sequence	Off-Cloud	On-Cloud	Difference
I5041	849	804	45 ± 41
I5046	932	858	74 ± 42
I5064	872	790	82 ± 41
I5067	1011	984	27 ± 45
I5070	617	580	37 ± 35
I10754 (filter)	5454	5355	99 ± 104
<b>All Comparison Fields</b>	<b>9735</b>	<b>9371</b>	<b>364 ± 138</b>
<b>I7229</b>	<b>1641</b>	<b>1560</b>	<b>81 ± 57</b>

Again, the pulse height distributions of the two regions are compared, both for the I7229 data and for the comparison regions. Again, for this comparison to be useful, only those comparison fields that have a proportional counter gain close to that of I7229 can be used. Since I7229 is a "high gain" observation (ALP=16), I5041, I5067 and I10754 can be used.

Figure 5 shows the pulse height distributions from the I7229 (L409) On-Cloud and Off-Cloud regions, and Figure 6 shows the pulse height distributions for the high-gain comparison fields. It appears that the pulse height distributions from the L409 On-Cloud region show a significant decrease in counts in channels 2-5 relative to the L409 Off-Cloud region - a decrease that is not found in the pulse height distributions from the comparison fields. This region of the sky will be closely examined with the ROSAT satellite, so see if this hint of absorption of the x-ray background by an interstellar cloud can be confirmed.



## B. Serendipitous Sources

### 1. H9191

A serendipitous source found in the image I3809 had an IPC count rate of  $0.058 \pm 0.001$  counts  $s^{-1}$ , which implies its flux is  $\approx 1.2 \times 10^{-12}$  erg  $cm^{-2}$   $s^{-1}$ , and its luminosity is  $\approx 1.4 \times 10^{28}$  ergs  $s^{-1}$  if its distance is 10 pc. The IPC coordinates of the source were given as  $12^h 25^m 41.8^s$ ,  $-63^\circ 4' 47''$  (1950) with a probable error of 1 arcminute. A finding chart was prepared by making a Polaroid picture of ESO plate 95 centered at the above coordinates and an optical candidate for the x-ray source was identified. A star of magnitude 9.2 was found at coordinates  $12^h 25^m 34^s$ ,  $-63^\circ 4' 24''$  (1950) and was identified as CPD 62°2774. Its spectral type is not given.

The follow up observation of this star by the HRI was obtained on 23 January 1981 between UT 05:27:40 and UT 06:04:32 and the data were returned as sequence number H9191. The observation yielded a "time in processed image" of 2194 seconds. A non-variable point source was found at  $12^h 25^m 36^s$ ,  $-63^\circ 4' 23''$  (1950), within 3 arcseconds of the position of the star CPD 62°2774. After subtracting background and allowing for electronics dead time, telescope vignetting, mirror scattering, and detector quantum efficiency, the HRI count rate was  $0.065 \pm 0.008$  counts  $s^{-1}$ . Figure 7 shows the HRI image of the CPD 62°2774 region.

### 2. H9192

The initial IPC observation of the O4f star 9 Sgr, sequence number I3124, detected it with an IPC count rate of  $0.045 \pm 0.004$  counts  $s^{-1}$ , which implies a flux of  $(9 \pm 1) \times 10^{-13}$  erg  $cm^{-2}$   $s^{-1}$  and a luminosity of  $(2.7 \pm 0.3) \times 10^{32}$  ergs  $s^{-1}$  at its distance of 1600 pc. The observation also revealed that 9 Sgr was surrounded by what appeared to be diffuse emission. Since 9 Sgr is a member of the Sgr OB1 stellar association, NGC 6530, it is also possible that what


appears to be diffuse emission is actually the superposition of emission by other stars in the OB association. There are two stars earlier than B0 and brighter than  $7.5^m$  within 10 arcminutes of 9 Sgr and three other stars brighter than  $10^m$  within 10 arcminutes. A follow up observation of 9 Sgr using the *Einstein* HRI was performed to determine if the other early-type stars in the field of view were also sources of x-rays, or if the additional emission was truly diffuse.

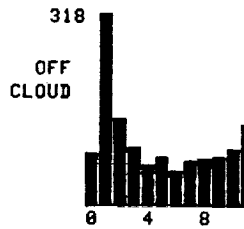
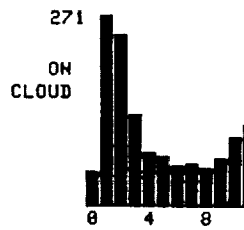
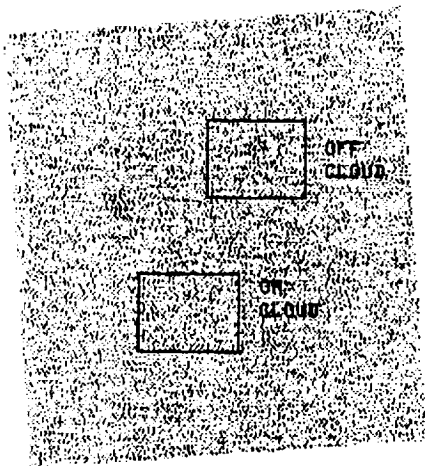
The follow up observation was performed on 24 March 1981 between UT 12:42:52 and UT 18:10:33 and the data were returned as sequence number H9192. The observation yielded a "time in processed image" of 7905 seconds. A possibly variable point source was found at  $18^h 0^m 48^s$ ,  $-24^\circ 21' 48''$  (1950) within 6 arcseconds of the position of 9 Sgr. After subtracting background and allowing for electronics dead time, telescope vignetting, mirror scattering, and detector quantum efficiency, the HRI count rate was  $0.031 \pm 0.005$  counts  $s^{-1}$ . The HRI image of the 9 Sgr region is shown in Figure 8.

No other point sources are apparent within 10 arcminutes of 9 Sgr. One other source is present more than 15 arcminutes from 9 Sgr at  $18^h 2^m 7^s$ ,  $-24^\circ 24' 14''$  (1950), within 4 arcseconds of the O6.5 V star HD165052, and has a corrected count rate of  $0.011 \pm 0.003$  counts  $s^{-1}$ . Thus, if the superposition of emission from point sources in the Sgr OB1 association is responsible for the diffuse emission seen in sequence number I3124 around 9 Sgr, those point sources are numerous and so weak that they are below the threshold for point source detection by this observation. That threshold is an x-ray luminosity of  $\approx 10^{32}$  ergs  $s^{-1}$ . Alternatively, a possible candidate is the emission generated in the shocked region where the stellar winds from 9 Sgr and other early type stars in the OB association interact with the nebulosity (cloud) near the OB association. Figure 9 shows a smoothed version of the H9192 image with the point sources removed, which lends some support to the latter interpretation.

## DIFFICULTIES ENCOUNTERED

The goal of this project was to use the *Einstein* satellite to look for absorption by dark interstellar clouds of the low energy x-ray diffuse background. The analysis procedure involves examining structure in the background regions of the image, rather than using the standard *Einstein* software to analyze x-ray point sources. This required writing a number of custom programs to further process the data to eliminate effects that were not very important for point source analysis, but which were crucial to diffuse data analysis. These custom programs were quite cumbersome and time-consuming to run. At some point, the *Einstein* team decided to reprocess the data base, and in so doing, they would do automatically (and probably better) much of the work that I was forced to do manually. I paused until the reprocessing was completed on the observations of interest before continuing my analysis. The analysis complications resulted in more trips to Cambridge than I had originally anticipated and delayed the final results. Figure 10 is a copy of a letter from the Center for Astrophysics to *Einstein* data users which confirms that the IPC reprocessing was not completed until June 1986.

BEINSTEIN OBSERVATORY  
I7237.IMG SEQUENCE: 7237  
SECONDS: 11370.  
RA, DEC: 97.500 10.667  
INSTRUMENT ROLL: 85.862  
TOTAL COUNTS: 29675.  
10 ARC-MIN:   
OBSERVER: SANDERS  
88-Nov-85



ORIGINAL PAGE IS  
OF POOR QUALITY

FIGURE 1

Chart 17237

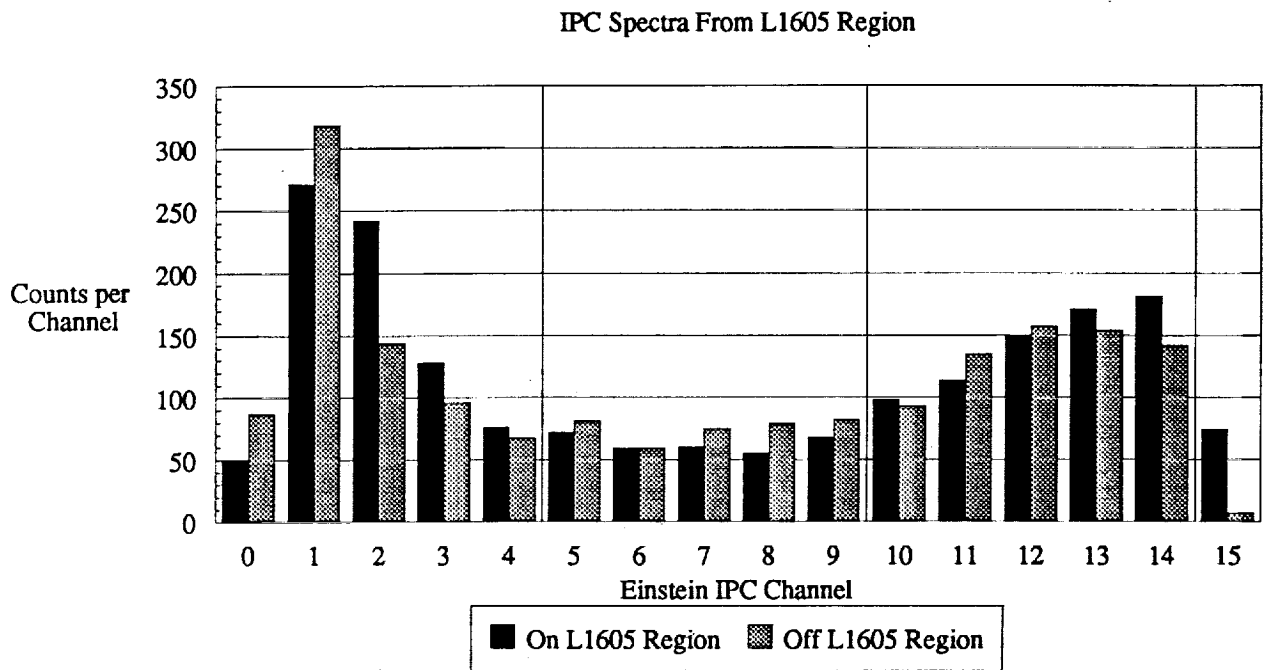


Figure 2

Chart HiAlp->I7237

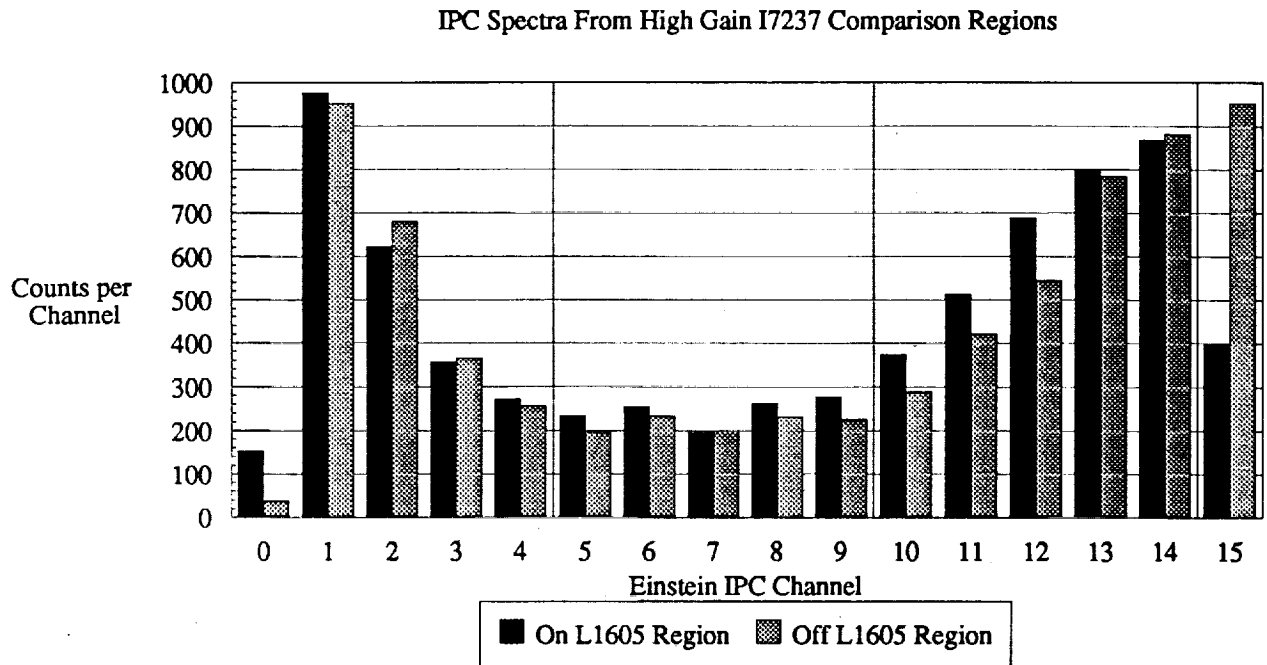
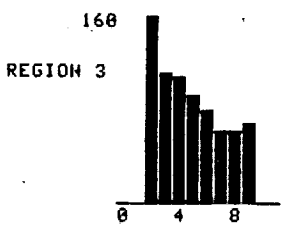
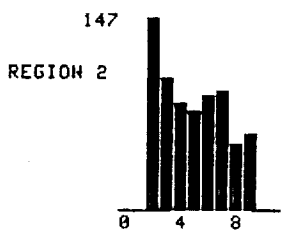
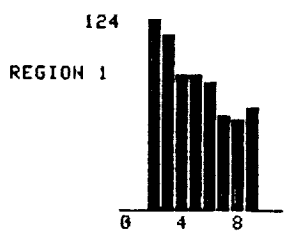
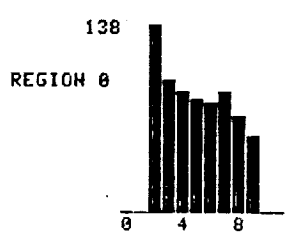
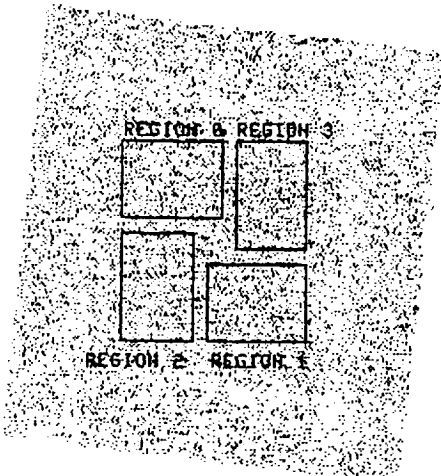


Figure 3

EINSTEIN OBSERVATORY  
 I7229.IMG SEQUENCE: 7229  
 SECONDS: 9594.  
 RA, DEC: 279.749 -13.508  
 INSTRUMENT ROLL: -83.848  
 TOTAL COUNTS: 25442.  
 18 ARC-MIN:  $\left| \begin{array}{c} \text{---} \\ \text{---} \end{array} \right|$   
 OBSERVER: GSFC  
 08-Nov-85



ORIGINAL PAGE IS  
 OF POOR QUALITY

FIGURE 4

IPC Spectra From L409 Region

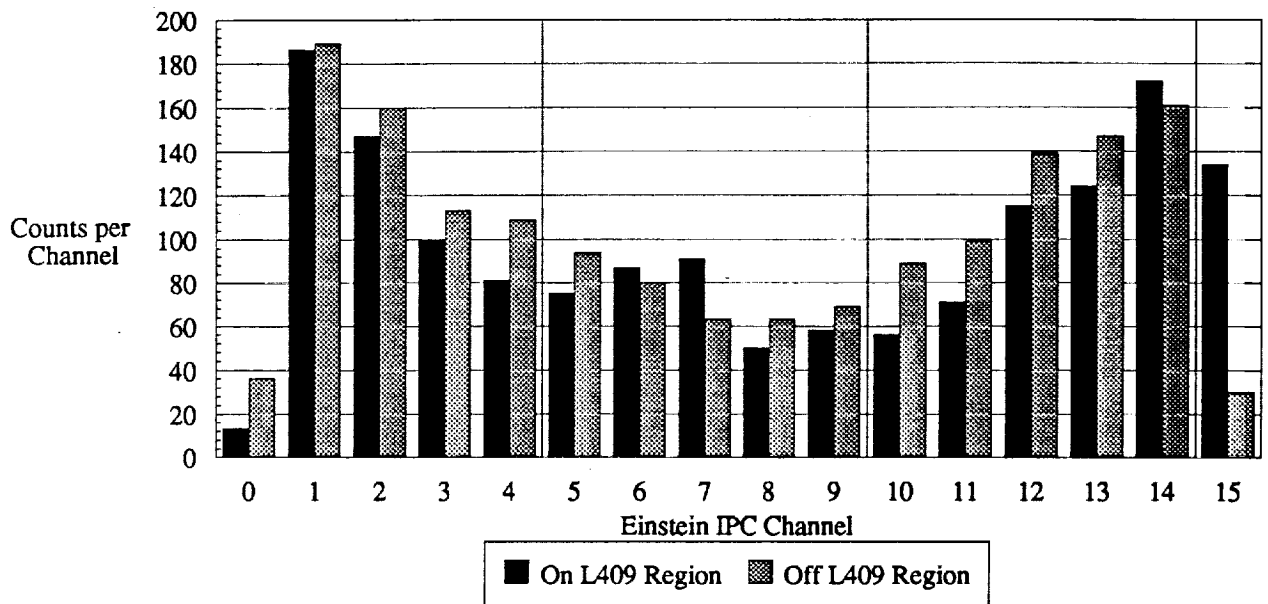


Figure 5



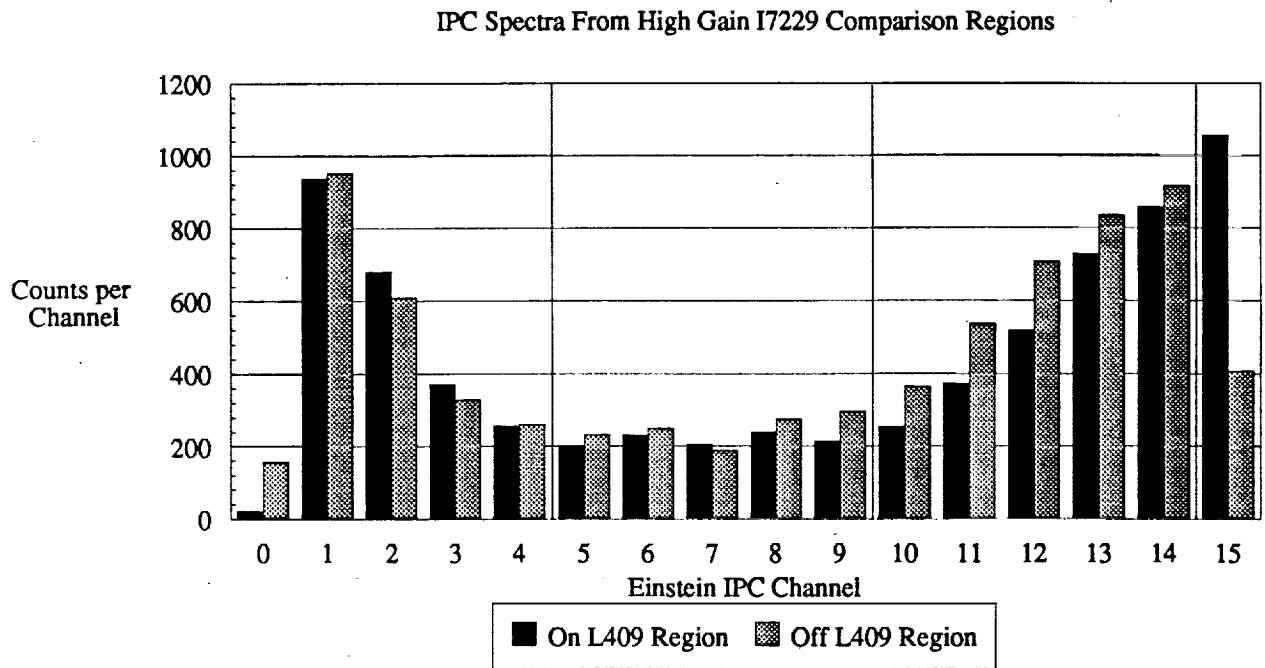
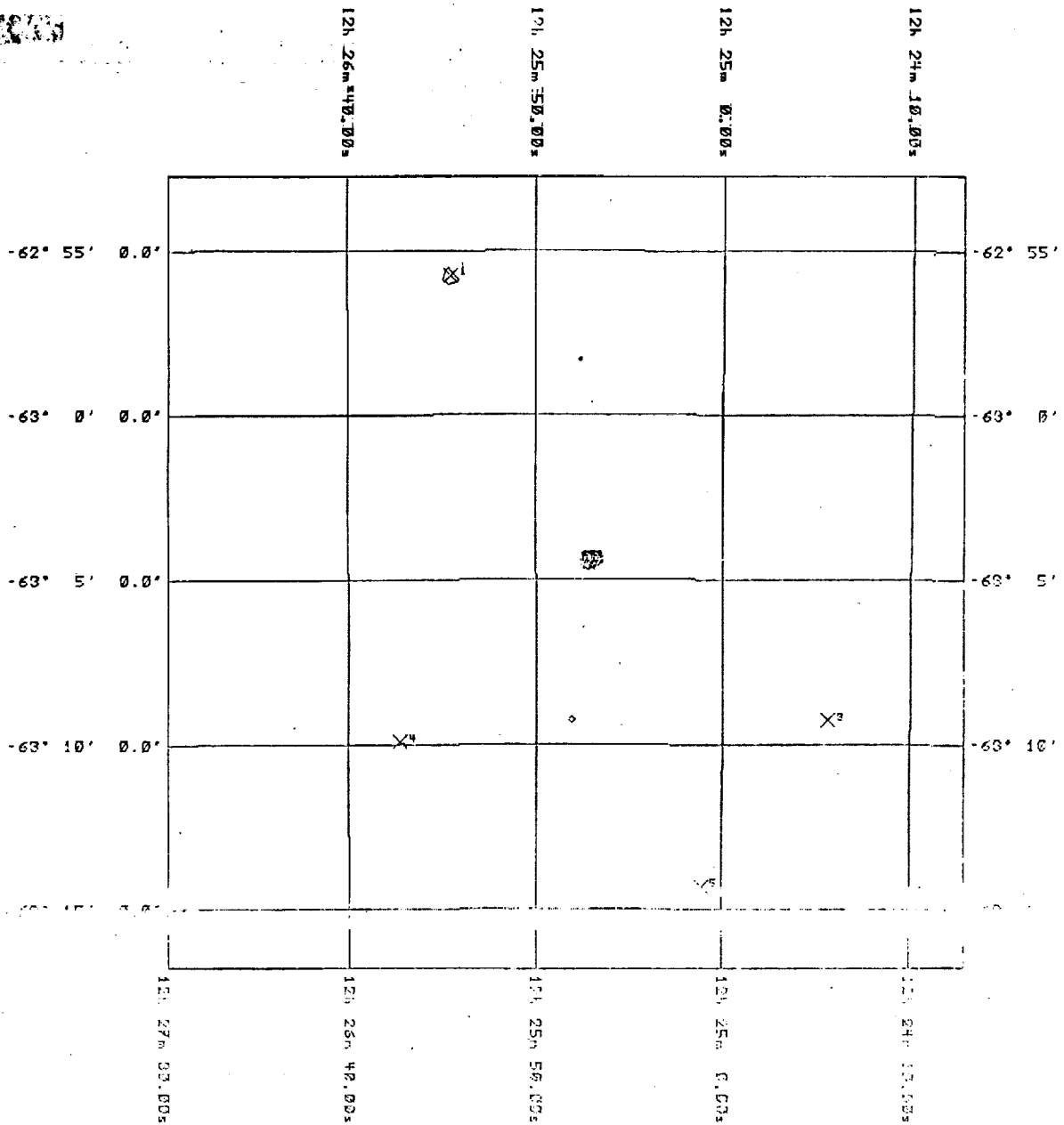


Figure 6



FWHM BEAM SIZE FOR HRI

ORIGINAL PAGE IS  
OF POOR QUALITY

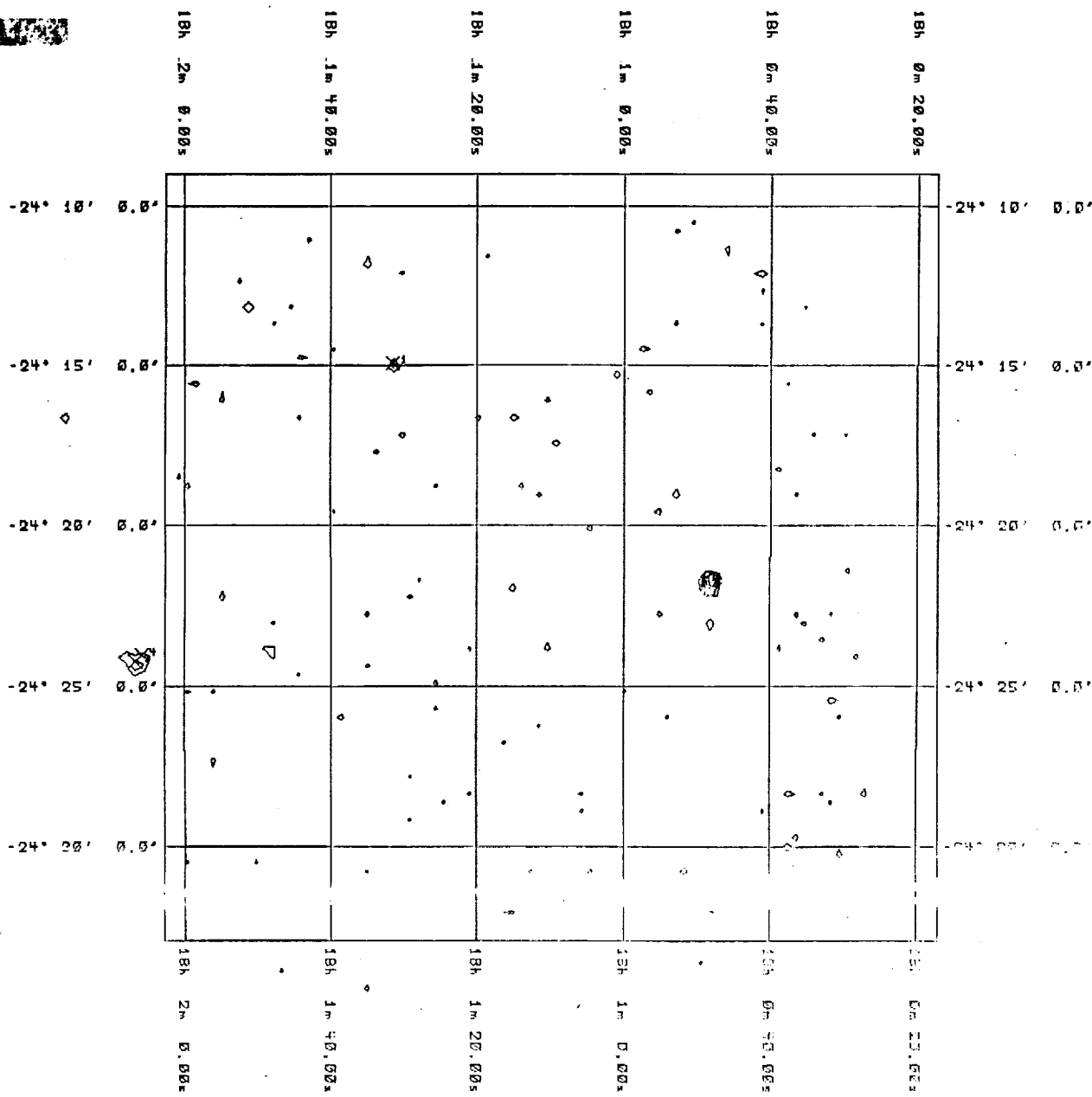
CONTOUR DATA FROM FILE H9191.IMG  
 ARRAY ELEMENTS: 128  
 PIXELS/ELEMENT: 32  
 VALUES RANGE FROM: 0 TO 86  
 NON-ZERO ELEMENTS: 3618  
 9 CONTOUR LEVELS:

	4.1	8.1	13.7	21.1	30.2	41.2	54.1	68.8	85.0
MAP CENTER:	186.42480	-63.07953			12h 25m 41.95s	-63d 47' 46.9"			
IMAGE CENTER:	186.42490	-63.07957			12h 25m 41.97s	-63d 47' 46.9"			
ROLL ANGLE:	.000								
MAP SCALE:	.0553 DEGREES/INCH								
	7.6740 ARC-SEC/MM								

SOURCES FROM SDF FILE H9191.SDF

SOURCE #	Y(ARC)	Z(ARC)	P.A.(Deg)	Dec.	P.A.(h.m.s)	Dec.(d.m.s)	Intensity
1	1829.67	962.04	126.55	-62.00	12h 26m 12.74s	-62d 47' 40.0"	4.17
2	2126.33	2000.15	126.40	-62.07	12h 25m 36.10s	-63d 47' 39.0"	2.17
3	2007.00	2285.95	126.13	-63.15	12h 27m 01.70s	-63d 47' 49.0"	1.01
4	1449.64	2602.25	126.61	-63.17	12h 26m 26.50s	-63d 47' 49.0"	3.22
5	2533.95	3131.74	126.27	-63.24	12h 26m 5.50s	-63d 47' 49.0"	1.22
6	2123.33	2014.62	126.40	-63.07	12h 25m 36.10s	-63d 47' 39.0"	2.17

FIGURE 7



FWHM BEAM SIZE FOR HRI

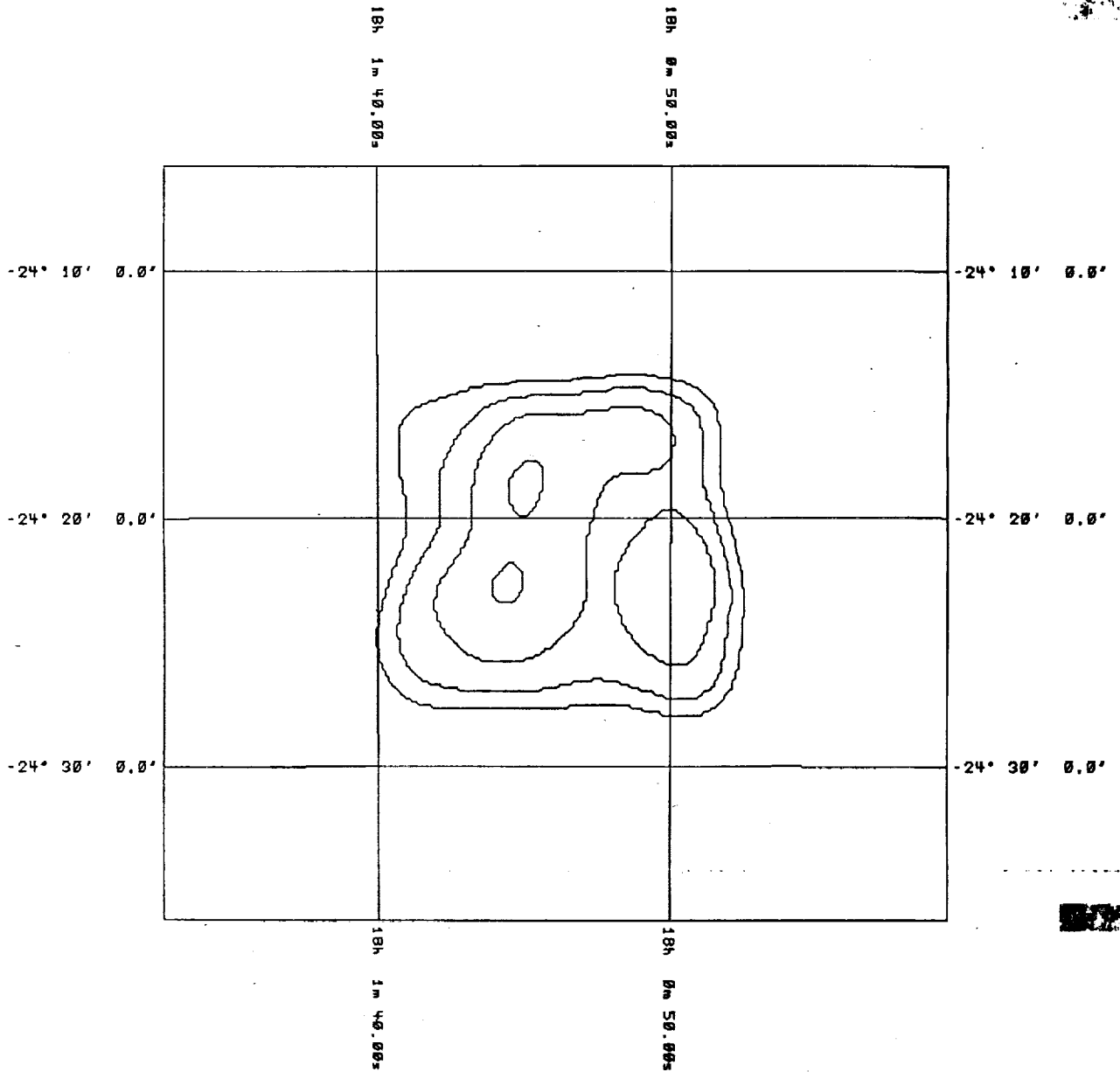
CONTOUR DATA FROM FILE H9192.IMG  
 ARRAY ELEMENTS: 128  
 PIXELS/ELEMENT: 32  
 VALUES RANGE FROM: 0 TO 89  
 NON-ZERO ELEMENTS: 7655  
 8 CONTOUR LEVELS:  
 7.1 12.3 19.3 28.1 38.7 51.1 65.4 81.6  
 MAP CENTER: 270.29000 -24.34995  
 IMAGE CENTER: 270.29100 -24.34995  
 ROLL ANGLE: .000  
 MAP SCALE: .0556 DEGREES/INCH  
 7.8740 ARC-SEC/MM

ORIGINAL PAGE IS  
 OF POOR QUALITY

SOURCES FROM SDF FILE H9192.SDF

SOURCE #	Y(px)	Z(px)	R.A.(deg.)	Dec.	R.A.(h.m.s)	Dec(d.m.s)	Intensity
1	1455.36	1320.35	270.38	-24.25	18h 1m 01.49s	-24d 14' 54.1"	1.00
2	2632.75	2144.57	270.20	-24.30	18h 0m 48.42s	-24d 01' 46.0"	10.00
3	501.28	2437.31	270.53	-24.40	18h 2m 06.44s	-24d 04' 14.0"	1.00
4	529.01	2410.94	270.52	-24.40	18h 2m 05.64s	-24d 04' 01.4"	1.1

FIGURE 8



FWHM BEAM SIZE FOR HRI

CONTOUR DATA FROM FILE H9192.Z16.Z888  
 ARRAY ELEMENTS: 128  
 PIXELS/ELEMENT: 16  
 VALUES RANGE FROM: 41 TO 81  
 NON-ZERO ELEMENTS: 16384  
 4 CONTOUR LEVELS:  
 65.1 70.1 75.1 80.1  
 MAP CENTER: 270.29080 -24.34995  
 IMAGE CENTER: 270.29100 -24.34995  
 ROLL ANGLE: .0000  
 MAP SCALE: .0706 DEGREES/INCH  
 10.0000 ARC-SEC/MM

18h 1m 9.84s -24d 20' 58.8"  
 18h 1m 9.86s -24d 20' 59.8"

ORIGINAL PAGE IS  
 OF POOR QUALITY

FIGURE 9